Scientia Iranica B (2014) 21(6), 1870–1879

SCIENTIA IRANICA

Sharif University of Technology
Scientia Iranica
Transactions B: Mechanical Engineering
www.scientiairanica.com

Estimation of local heat transfer coefficient in impingement jet by solving inverse heat conduction problem with mollified temperature data

S.D. Farahani[a,*], F. Kowsary[a] and J. Jamali[b]

a. *Center of Excellence in Design and Optimization of Energy Systems, School of Mechanical Engineering, College of Engineering, University of Tehran, Tehran, Iran.*
b. *Department of Mechanical Engineering, Shoushtar Branch, Islamic Azad University, Shoushtar, Iran.*

Received 21 July 2012; received in revised form 8 March 2014; accepted 8 April 2014

KEYWORDS
Heat transfer coefficient;
Impingement jet;
Sequential function specification method;
Conjugate gradient method;
Mollification method.

Abstract. The aim of this paper is to determinate local convective heat transfer coefficient slot jet impingement using inverse heat conduction methods. The sequential specification function method and the conjugate gradient method are used to solve the Inverse Heat Conduction Problem (IHCP) and estimate the space-variable convective heat transfer coefficient. This paper proposes a procedure to smooth the temperature data by the mollification method prior to utilizing the inverse method. The measured transient temperature data may be obtained from locations inside the body or on its inactive boundaries. The uncertainties in the estimated heat transfer coefficient are calculated using bias and variance errors. The obtained results show that mollifying measured data causes an increase in the accuracy and stability of the estimation.

1. Introduction

Jet impingement is widely used in industry because of the highly favorable heat transfer rate it provides. Engineering applications include annealing of metal sheets, drying of textile products, deicing of aircraft wings, and cooling of gas turbine blades and electronic components. A case of special interest is the impingement of a turbulent slot jet on a flat plate. Figure 1 shows a schematic of different zones in this type of jet impingement. Earlier experimental studies have shown that the length of the jet potential core is typically between five to seven slot widths, and that the maximum heat transfer occurs when the transitional jet hits the plate [1,2]. Mass transfer methods have been widely used for many years. The heat-mass transfer analogy, in conjunction with the naphthalene sublimation technique, was used to investigate local and average heat transfer coefficients in a two-row plate fin and tube heat exchanger with circular tubes [3]. The local mass transfer coefficients on this geometry have also been measured by Krückels and Kottke [4]. They used a chemical method based on absorption, chemical reaction and coupled color reaction [5]. The solid surface is coated with a wet filter paper, and the ammonia to be transferred is added as a short gas pulse. The locally transferred mass is visible as color density distribution and the color intensity corresponds to the local mass flow. Thermo chromic liquid crystals have been applied extensively to heat transfer measurements [6-7]. Using temperature maps obtained from liquid crystals applied to a constant heat flux surface, Newton's law of cooling (the boundary condition of the third kind) is used to establish distributions of the convective heat transfer coefficient. A constant

*. *Corresponding author. Tel.: +98 21 61114024; Fax: +98 21 88013029*
E-mail address: sdavoodabadifarahani@gmail.com (S.D. Farahani)

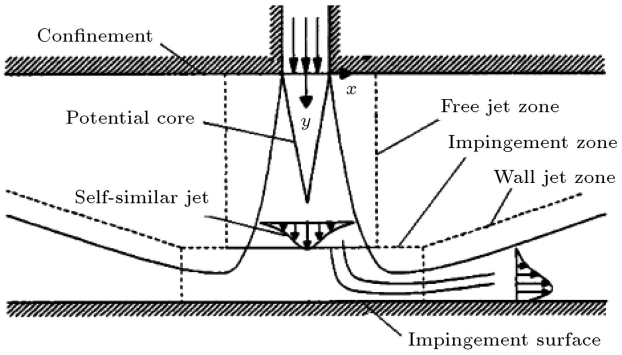

Figure 1. Schematic of a turbulent slot jet impinging on a flat surface.

heat flux at the body surface is typically generated by passing an electrical current through a fin film with uniform electrical resistivity. Thermo graphic phosphors have also been used for local heat transfer measurements [8,9]. Application of temperature sensitive paints to heat transfer measurements is described by Liuo and Sullivan [10]. Optical measurement techniques have found widespread application in heat transfer investigations [11,12]. Differential interferometry can be used to determine local temperature gradients in the fluid and a local heat transfer coefficient at the solid surface.

However, these methods either require expensive or delicate equipment or have limitations to high temperatures or high levels of turbulence in the flow. An alternative method that is also particularly suited for the investigation of impingement jet heat transfer is the Inverse Heat Conduction (IHC) technique. It is advantageous because it can be carried out with simple, low-cost instrumentation and subsequent numerical procedures. In this technique, temperatures measured at some proper interior locations are used to estimate a thermal boundary condition. The word "estimation" is used here as temperature measurements always contain noise. The Inverse Heat Conduction Problem (IHCP) is mathematically "ill-posed" in the sense of Hadamard [13], and this causes the IHCP to be particularly sensitive to measurement errors. The IHCP can be classified according to factors, such as (1) linearity, (2) the time domain used (sequential vs. whole domain), and (3) dimensionality. Many investigators have developed various inverse schemes over the past 40 years. Tikhonov's regularization technique [14] and Beck's function estimation method [15] are among the most well-known approaches in inverse heat transfer. Another method that has been widely used is the conjugate gradient method (see, e.g. [16]), which belongs to the class of iterative regularization techniques. Masson et al. [17] applied iterative regularization and Function Specification Methods (FSMs) with a spatial regularization to estimate the two-dimensional heat transfer coefficient. Taler [18] compared two techniques, Singular Value Decomposition (SVD) and Levenberg-Marquardt used in determining the space variable heat transfer coefficient on a tube circumference. Good agreement was found between the results in a simulated experiment. Guzik and Styrylska. proposed the generalized optimal dynamic filtration method, developed on the Unified Least-Squares Method (ULSM) with the use of the multistage-multi group (M-M) technique, for the mathematical modeling of transient temperature fields, using data subject to uncertainties [19]. Kowsary and Farahani [20] applied denoised measurement data using the mollification method before the standard IHCP algorithm for estimated heat flux for classical inverse problems. The purpose of this study is to use the solution of a transient, sequential IHC scheme (sequential function specification method) [13] and iterative scheme (conjugate gradient method) [16] with and without denoised data, using the mollification method, to estimate distribution of the steady-state convective heat transfer coefficient in a slot jet impingement. The method is required to be considered two-dimensional because of the lateral conduction that occurs between the warmer and cooler areas of the surface of the target plate, which, in many investigations using a thermocouple, was disregarded. Due to the existence of lateral conduction within stainless steel, the local heat transfer coefficient was corrected to include this effect. The correction was performed regarding a two-dimensional model.

The mollification method is used for smoothing the simulated measurement in simulation for estimation of the heat transfer coefficient.

2. Problem description

To use the inverse scheme, firstly, the direct problem should be formulated. The governing differential equation is the following two dimensional transient heat conduction equations solved in the mid-plane ($z = 0$) of the target plate (Figure 2). Assuming constant thermal

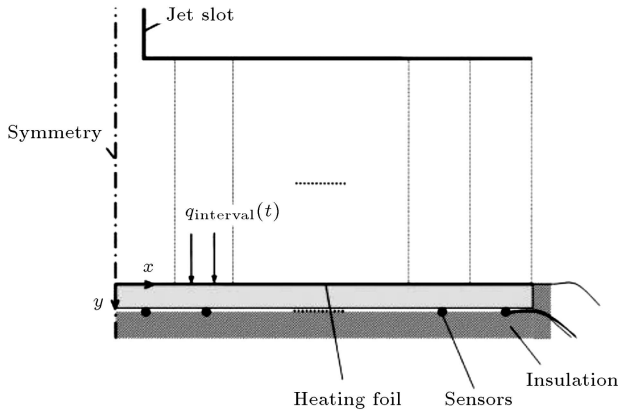

Figure 2. Schematic of the experiment set-up for inverse method.

properties:

$$\frac{\partial^2 T}{\partial x^2}+\frac{\partial^2 T}{\partial y^2}=\frac{1}{\alpha}\frac{\partial T}{\partial t},$$

$$\frac{\partial T}{\partial x}|_{x=0}=\frac{\partial T}{\partial x}|_{x=L_1}=\frac{\partial T}{\partial y}|_{y=L_2}=0,$$

$$-k\frac{\partial T}{\partial y}|_{y=0}=q(x,t) \quad \text{and} \quad T|_{t=0}=T_0, \tag{1}$$

where T_0 is the initial temperature of the plate (= room/surrounding temperature), and L_1 and L_2 are half-plate length and plate thickness, respectively. In the inverse problem, the boundary condition on the top ($y = 0$) surface, $q(x,t)$, is unknown; instead, some temperature measurements at discrete times and locations are given:

$$Y_{j,i}=T_{\text{meas}}(x_j,t_i), \tag{2}$$

where i and j are measurement time and number of sensor indices, respectively. In the estimation of the heat transfer coefficient, two approaches can be used: (a) the direct estimation and (b) the estimation of $q(x,t)$, subsequent calculation of $T_{\text{surf}}(x,t)$, and then using Newton's law of cooling. While direct estimation might seem more appealing, the second approach causes the IHCP to remain linear, thus, eliminating the need for iteration, which accelerates the solution considerably. Note that in the present set-up, a heating foil generates a constant known heat flux of Q_s on the top surface. A part of Q_s, namely $q(x,t)$, is conducted into the solid and estimated by the IHCP. The heat transfer coefficient is then calculated using the remaining part, which is carried away by the jet, using Newton's law of cooling:

$$h(x)=\frac{Q_s-q(x,t)}{T_{\text{surf}}(x,t)-T_{\text{jet}}}, \tag{3}$$

where $T_{\text{surf}}(x,t)$ and T_{jet} are the top surface and the jet exit temperatures, respectively. For solving the inverse heat conduction problem, two methods were employed, namely, the Sequential Function Specification Method [13] and the Conjugate Gradients Method [16].

The differential equation for X is obtained from the direct differentiation of the governing heat conduction equation with respect to q. This way of calculating X is particularly suited for this study, since, in the presence of linearity, sensitivity coefficients will be independent of unknown parameters, that is, once calculated, they remain constant in the course of the inverse procedure. Based on this description, the sensitivity equations are as follows:

$$\frac{\partial^2 X}{\partial x^2}+\frac{\partial^2 X}{\partial y^2}=\frac{1}{\alpha}\frac{\partial X}{\partial t},$$

$$\frac{\partial X}{\partial x}|_{x=0}=\frac{\partial X}{\partial x}|_{x=L_1}=\frac{\partial X}{\partial y}|_{y=L_2}=0,$$

$$-k\frac{\partial X}{\partial y}|_{y=0}=\begin{cases}1 & x_n<x<x_{n+1}\\ 0 & \text{otherwise}\end{cases}, X|_{t=0}=0 \tag{4}$$

3. Method description

3.1. The Conjugate Gradients Method (CGM)

In order to estimate the heat flux using the conjugate gradients method, the error function S is also defined as:

$$S(q)=\sum_{i=1}^{N_s}\sum_{m=1}^{N_m}\left(T_i(t_m)-Y_i(t_m)\right)^2, \tag{5}$$

where Y is measured temperatures at the sensor location and T is the estimated value at the sensor location. In Eq. (5), NS refers to the number of temperature sensors. The directional derivative of S can be used to define the gradient function of ∇S, with respect to Q, as follows:

$$\vec{\nabla}S=-2[X]^T\left([Y]-[T]\right), \tag{6}$$

where all the mentioned parameters are evaluated at the sensor location. Using the above equation, the conjugate direction (d) can be calculated as:

$$d^k=\nabla S(Q^k)+\gamma^k d^{k-1}. \tag{7}$$

The conjugate coefficient, γ, is calculated as:

$$\gamma^k=\left(\int_{t=0}^{t_f}\{\nabla S(Q^k)\}^2dt\right)/\left(\int_{t=0}^{t_f}\{\nabla S(Q^{k-1})\}^2dt\right), \tag{8}$$

where $\gamma^0=0$. If $Q'=Q^k+d^k$ is substituted in Eq. (1), then, values ΔT will be calculated at the sensor location, as follows:

$$\Delta T=T(Q')-T(Q^k). \tag{9}$$

Therefore, the search step size (β) can be obtained as:

$$\beta^k=\left(\sum_{j=1}^{J}\sum_{m=1}^{M}\left(T_j(t_m)-Y_j^m(t_m)\right)\Delta T_j(t_m)\right)/\left(\sum_{j=1}^{k}\sum_{m=1}^{M}\Delta T_j^2(t_m)\right). \tag{10}$$

In this method, an iterative procedure is used to estimate the imposed heat flux. This iterative method can be summarized by the following equation:

$$Q^{k+1} = Q^k - \beta^k d^k, \tag{11}$$

where "d" is a conjugate direction and β is the search step size. The computational procedure for the solution of this inverse problem may be summarized as follows:

Suppose Q^n is available at iteration n.

Step 1. Solve the direct problem given by Eq. (1) for T.

Step 2. Examine the stopping criterion, considering $S(Q) < \alpha$, where α is a small-specified number. Continue if not satisfied.

The "Discrepancy Principle" method in the conjugate gradient method has been used in this study. In this method, the iterations are terminated prematurely when the following criterion is satisfied [16]:

$$S(Q) < \alpha. \tag{12}$$

In this case, the iterations are stopped when the residuals between measured and estimated temperatures are of the same order of magnitude as the measurement errors. That is:

$$|Y(t) - T(X,t)| < \sigma \quad \text{(i.e. standard deviation)}. \tag{13}$$

Step 3. Solve the sensitivity equation given by Eq. (4) for X.

Step 4. Compute the gradient of the functional ∇S from Eq. (6).

Step 5. Compute the conjugate coefficient, γ^k, and direction of descent, d^k, from Eqs. (7) and (8), respectively.

Step 6. Set $\nabla Q = d^k$ in Eq. (1), and solve for calculated ΔT.

Step 7. Compute the search step size, β^k, from Eq. (10).

Step 8. Compute the new estimation for Q^{n+1} from Eq. (11) and return to Step 1.

3.2. The Sequential Function Specification Method (SFSM)

This inverse method is sequential and uses Beck's function specification approach, where heat fluxes of r "future" time steps are temporarily assumed constant and used to add stability to the estimations. It is assumed that heat fluxes from time $1, 2, .., (m-1)$ are estimated, and now the unknowns in time m are to be evaluated. The standard form of the IHCP is the matrix equation (see [13]):

$$T = T|_{q=0} + Xq, \tag{14}$$

where $T|_{q=0}$ is the calculated temperatures at sensor locations from the solution of the direct problem using $q_1, ..., q_{m-1}$ and setting Eq. (7a) to zero for Np heat flux parameters, Ns temperature sensors, and r future times:

$$T = \begin{bmatrix} T(m) \\ T(m+1) \\ \vdots \\ T(m+r-1) \end{bmatrix} \quad \text{and} \quad T(i) = \begin{bmatrix} T_1(i) \\ \vdots \\ T_2(i) \\ \vdots \\ T_{\mathrm{Ns}}(i) \end{bmatrix}, \tag{15}$$

where T is an Ns.$r \times 1$ matrix:

$$q = \begin{bmatrix} q(m) \\ q(m+1) \\ \vdots \\ q(m+r-1) \end{bmatrix} \quad q(i) = \begin{bmatrix} q_1(i) \\ q_2(i) \\ \vdots \\ q_{\mathrm{Np}}(i) \end{bmatrix}, \tag{16}$$

where T is an Np.$r \times 1$ matrix, and:

$$Z = \begin{bmatrix} a(1) & & & \\ a(2) & a(1) & & \\ \vdots & \vdots & \ddots & \\ a(r) & a(r-1) & \cdots & a(1) \end{bmatrix}, \tag{17}$$

where Z is an Ns.$r \times$ Np.r matrix, and:

$$a = \begin{bmatrix} a_{11}(i) & a_{12}(i) & \cdots & a_{1\mathrm{Np}}(i) \\ a_{21}(i) & a_{22}(i) & \cdots & a_{2\mathrm{Np}}(i) \\ \vdots & \vdots & & \vdots \\ a_{\mathrm{Ns}1}(i) & a_{\mathrm{Ns}2}(i) & \cdots & a_{\mathrm{NsNp}}(i) \end{bmatrix},$$

$$a_{jp} = \frac{\partial T(x_j, t_i)}{\partial q_p}, \tag{18}$$

where $a(i)$ is a matrix of Ns $\times$ Np.

Note that there are Np unknown heat flux components at each time, t_m. There are Ns measurements at that time, and Ns must be no less than Np. To produce stable results, we use r matrix equations in a least squares method. The sum of squares of the difference between calculated and measured temperatures, in matrix form, is:

$$S = (Y - T)^t (Y - T), \tag{19}$$

with the temporary assumption of:

$$q_1(m) = q_1(m+1) = ... = q_1(m+r-1).$$

$$.....q_{\mathrm{Np}}(m) = q_{\mathrm{Np}}(m+1) = ... = q_{\mathrm{Np}}(m+r-1). \tag{20}$$

Here, the function to minimize is:

$$S = \left(Y - T|_{q=0} - Zq\right)^T \left(Y - T|_{q=0} - Zq\right), \tag{21}$$

where:

$$Z = XA; \quad A = \begin{bmatrix} A(1) \\ \vdots \\ A(r) \end{bmatrix}. \tag{22}$$

For a constant **q** assumption $A(i) = I_{\mathrm{Np}\times\mathrm{Np}}$ where I is unity matrix.

The matrix derivative of Eq. (20), with respect to q (in order to minimize S), yields the estimator equation:

$$\hat{q} = \left(Z^T Z\right)^{-1} Z^T \left(Y - T|q=0\right), \tag{23}$$

which gives the $\hat{q}(m)$ vector as defined by Eq. (14). The following estimation procedure is employed: X and, consequently, Z are calculated, and m is set to one. Estimation begins with the calculation of $T|_{q=0}$ using the direct problem and subsequent application of Eq. (22). Then, m is increased by one, $T|_{q=0}$ is recalculated, and the estimator equation is used again.

3.3. The mollification method

Use of the mollification method is discussed more thoroughly, as it is the central subject of this article. The mollification method is a regularization method that uses the averaging property of the Gaussian kernel to smooth noisy data. The automatic character of the mollification algorithm, which makes it highly competitive, is due to the incorporation of the Generalized Cross Validation procedure for selection of the radius of mollification as a function of the perturbation level in the data, which is generally not known. The mathematical form of the mollification method was detailed in Ref. [19] and will not be repeated here. Note that we used the mollification method as prefiltering for denoising measurement data before the inverse algorithm.

The impingement surface is divided into a number of sub-intervals (see Figure 2). The aim is to estimate the time-variable heat flux, $q_{\mathrm{interval}}(t)$, on each interval and subsequent calculation of the local convective heat transfer coefficient. The inverse methods employed are sequential and use Beck's function specification approach and conjugate gradient method. The key factors in an experimental design are measurement time-step size. Minimizing the time steps, for example, causes measurement errors to become correlated, which introduces instability into the results. High correlation between temperature data implies that each new measurement is providing less information than if the correlation was zero. Bias (index of deviation from the actual value), variance (index of intensity of fluctuations), and sensitivity coefficients are good judgment parameters in determining the best experimental set-up. The final target of the estimations is the heat transfer coefficient on each interval. For each interval, bias (D) is defined for the IHCP as:

$$D = \sqrt{\frac{1}{N}\sum_{i=1}^{N}\left(\hat{h}_{i,\mathrm{nonoise}} - h_{i,\mathrm{true}}\right)^2}, \tag{24}$$

where $\hat{h}_{i,\mathrm{nonoise}}$ noise is the estimated heat flux using the measurements containing no noise. The Root Mean Square (RMS) error is also calculated by:

$$\mathrm{RMS} = \sqrt{\frac{1}{N}\sum_{i=1}^{N}\left(\hat{h}_{i,\mathrm{noisydata}} - h_{i,\mathrm{true}}\right)^2}, \tag{25}$$

where $\hat{h}_{i,\mathrm{noisydata}}$ data is the estimated heat flux using the temperature data polluted with noise. Variance can then be determined by:

$$V = \mathrm{RMS}^2 - D^2. \tag{26}$$

A series of simulations is performed to ensure the ability of the inverse scheme in estimating the space variable heat transfer coefficient and to find the optimal simulation configuration. Only half of the plate is considered due to symmetry. This half-plate is 10-mm thick, 52.5-mm long (7 slot widths), stainless-steel (AISI 304), and insulated on the bottom and side surfaces (Figure 2). A functional form for the heat transfer coefficient is not known a priori, which is the case in many jet impingement heat transfer investigations. The fluid temperature, $T_{\mathrm{jet}} = T_\infty$, is also a known input to the inverse scheme. After the flow has reached the hydrodynamic steady state, a heat generation source initiates, and, simultaneously, temperature recordings are started using K-type sheathed thermocouples of 1.25-mm diameter. In the present investigation, the heat source is a heating foil applied to the top surface of the plate (when necessary, this source can be of any form; it only requires the appropriate reformulation of the direct problem), and the measurements are carried out at the bottom. This choice of sensor location is most favorable for the experiment's hardware design, since it is simpler in terms of installation; however, it is most challenging for the inverse scheme, since it is farthest from the active surface (resulting in more

"damped" and "lagged" temperature data due to the diffusive nature of heat conduction).

Experimental heat transfer coefficient data obtained from a confined slot jet impingement study [21] is employed, together with the finite element method, to produce the "measured" temperatures. In this paper, the finite element method is used in numerical solutions where ANSYS capabilities are utilized in the mesh generation and numerical solution of the problem, in order to evade the need for coding the direct heat conduction problem. By simulating the problem in the graphic user interface of the software and saving it in the form of a function, the numerical solution of the problem can be performed merely by calling the saved function. Inverse algorithms are written in ANSYS Parametric Design Language (APDL). The element type is Plane-55. A curve fitting of seven linear sections was applied to the experimental data of [21] to obtain the continuous heat transfer distribution. The temperatures at the sensor locations were obtained from the temperature histories at the bottom of the plate. In the inverse heat conduction problem, there are a number of measured quantities in addition to temperature, such as time, sensor location, and specimen thickness. Each is assumed to be accurately known except the temperature. The temperature measurements are assumed to contain the major sources of error or uncertainty. Any known systematic effects due to calibration errors, the presence of the sensor, conduction and convection losses, or whatever, are assumed to be removed to the extent that the remaining errors may be considered random. These random errors can then be statistically described. In this study, the inverse scheme used is tested using simulated measured temperatures containing Gaussian noise. The following standard assumptions were applied in generating measurement errors: they have a random, additive, and uncorrelated nature with zero mean and constant variance, and they have normal (Gaussian) distribution. Noise with $\sigma = 0.5$ was added to the temperature data.

4. Results and discussion

In this section, the results obtained from simulations are presented. This study emphasizes the use of IHC techniques and filtering for estimating the heat transfer coefficient. Among a number of parameter sets that were used for validation of the method, the data for Re=13,600 and $H/W = 8$ (H and W are the nozzle-to-plate distance and the slot width, respectively) are chosen for presentation of the results in which the flow type is turbulent, as the mentioned methods in the introduction either require expensive or delicate equipment or have limitations to high temperatures or high levels of turbulence in the flow. Note that this method is independent of the flow type, Re and H/W. This study is performed to ensure the ability of the inverse scheme in estimating the space variable heat transfer coefficient. Measurements are carried out until the plate reaches the thermal steady-state condition, which takes approximately 2 minutes. The half-plate is divided into seven equally spaced intervals (Np = 7), and seven sensors are installed at the bottom of the plate beneath each interval. As previously described, interval (t) is estimated for all intervals using the IHCP. $T_{\text{surf}}(x,t)$ is then calculated, and Eq. (3) is employed to determine $h(x)$. A test (by the mentioned inverse methods) is performed to demonstrate that the heat transfer coefficients are independent of the magnitude of the applied surface heat flux. Note that the "Exact" word in the figures means that the heat transfer coefficient for generation of measured temperature data is used, and the main aim of the mentioned algorithms is its estimation. The time-average heat transfer coefficient on each space interval of the surface is obtained from averaging the estimated heat transfer coefficient of that interval in time. Figure 3(a) and (b) illustrate the results for estimation of the heat transfer coefficient by the sequential function specification method and the conjugated gradient method, where different subjected surface heat fluxes were used in the numerical experiments. The deviation of results from the so-called "Exact" data is due to the nature of the inverse technique. Figure 3(b) illustrates that the CGM is more accurate than the SFSM. The figures show that the amount of q_s has no significant effect on the end results.

However, the bias is growing as well, which puts a limit on our choice of r. This trade-off between bias and variance often happens in inverse schemes. The decision concerning factors such as (r) or the time to make measurements is called simulation design. For the present set-up, $r = 3$ performs the best (see Table 1). A choice of time steps bigger than 1.4 sec is not advisable, as bias is also rapidly growing. In addition, it should be remembered that from the IHCP point of view, a significant amount of information is lost when we choose too-large time steps. Note that this choice of T_{meas} is for the present set-up. It is evident that if, for example, a more "responsive" material is used as the impingement plate (such as copper), then a much smaller time step would meet the criteria of experiment design. Time step 1.2 sec is chosen to

Table 1. Variation of bias and variance errors with increasing r in SFSM without mollified data.

r	Average bias in $h(x)$	Average variance in $h(x)$
3	2.696	20.2223
4	3.35	19.8
8	11.2	17.9

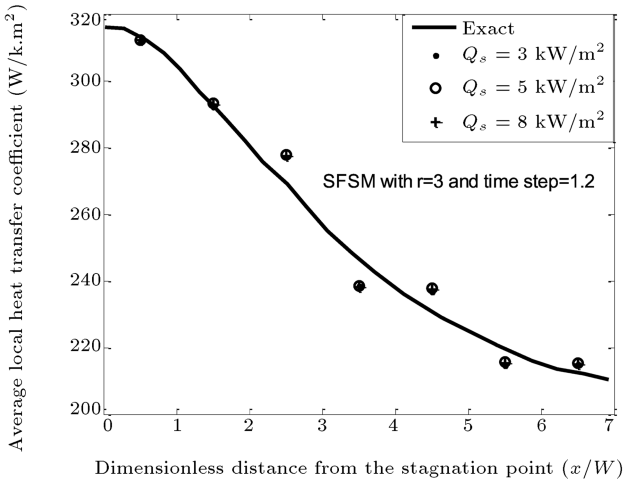

(a)

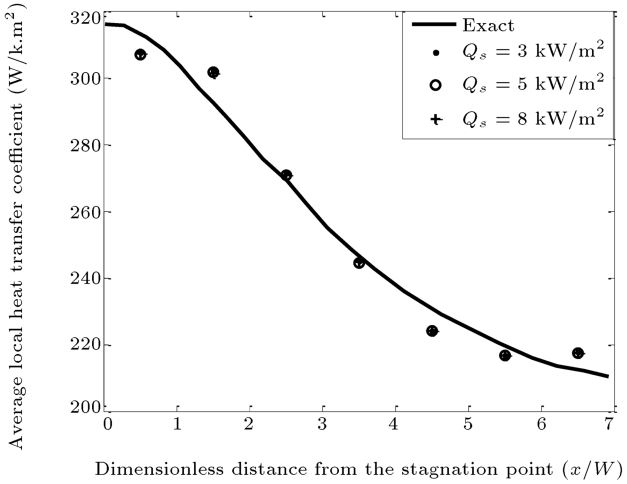

(b)

Figure 3. The estimation average local convective heat coefficient by using (a) Sequential Function Specification Method (SFSM) with various Q_s, and (b) conjugate Gradient Method (CGM) with various Q_s value.

perform. The heat transfer coefficient on each interval is constant and calculated in time using Eq. (3). The heat transfer coefficient on each interval in time is estimated using the sequential function specification method and the conjugate gradient method with time step 1.2 sec and stopping criterion $1e-6$, as shown by Figures 4 and 5, respectively. The fluctuations are the consequence of the noise present in the measurements. Earlier times are omitted, since they exhibit the most sensitivity to measurement errors. The effect of noise is also clear from the comparison of Figures 4 and 5. These figures show that by using the mollification method for smoothing measurement data before the IHC algorithm, fluctuations in the estimated parameter are reduced. As mentioned earlier, the final value for the heat transfer coefficient on each space interval of the surface is obtained from averaging the estimated

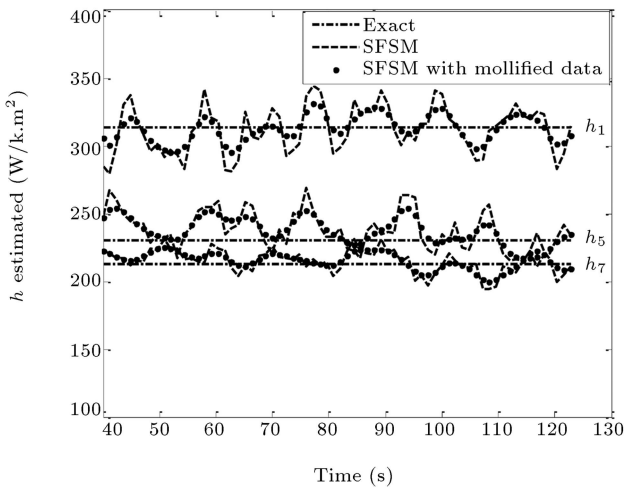

(a)

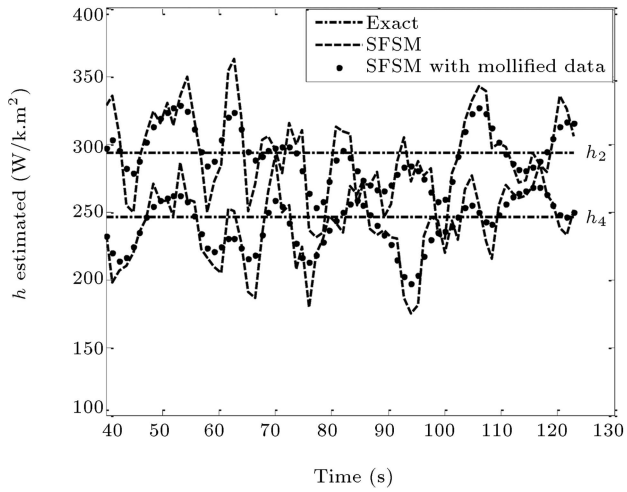

(b)

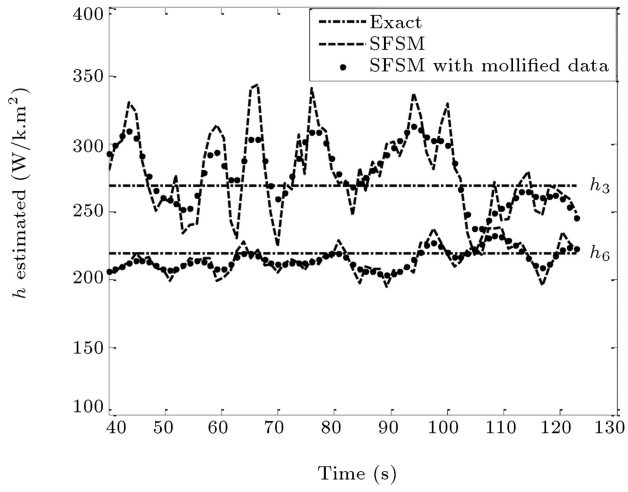

(c)

Figure 4. The estimated heat transfer coefficients: (a) h_1, h_5 and h_7, (b) h_2 and h_4, and (c) h_3 and h_6, in time by using Sequential Function Specification Method (SFSM) with and without mollified data.

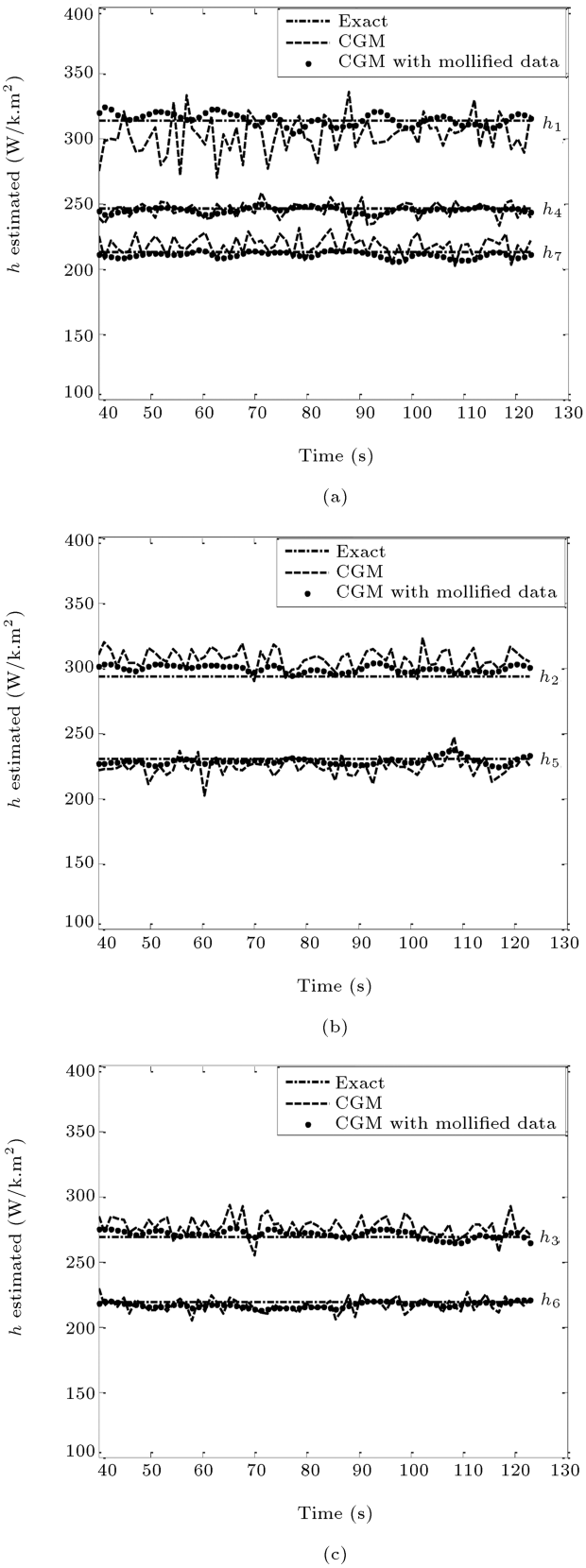

Figure 5. The estimated heat transfer coefficients: (a) h_1, h_4, and h_7, (b) h_2 and h_5, and (c) h_3 and h_6, in time by using Conjugate Gradient Method (CGM) with and without mollified data.

Table 2. Bias and variance errors in SFSM and CGM with and without mollified data.

Inverse method	Average RMS in $h(x)$	Average bias in $h(x)$	Average variance in $h(x)$
SFSM	20.6341	2.6960	20.2223
SFSM with mollified data	13.9746	2.8267	13.3748
CGM	10.4281	1.3205	10.2936
CGM with mollified data	7.4122	1.3541	7.1534

heat transfer coefficient of that interval in time. It is important that the time step for the mentioned algorithm with mollified data (0.7 sec) be smaller than that without mollified data (1.2 sec). By using the mollified data, we can choose small time steps and achieve more information regarding the estimated parameter.

Figure 3(a) and (b) illustrate the final results of estimations, when Q_s is 8 kW/m^2. Table 2 shows that the RMS value and the variance value are reduced when we use the mollified data. We understand from this table that the conjugate gradient is more accurate than the sequential function specification method. The estimation has the most sensitivity to errors in measurement data, but the mollified data has little error. In this method, we must measure only temperature by the thermocouple then use the inverse algorithm for estimation of the local heat transfer coefficient. Using an inverse scheme with mollified data for estimation of local heat transfer coefficient is a new idea for optimal experiment design.

5. Conclusion

The simulation set up presented in this study works efficiently using the inverse scheme to estimate the local convective heat transfer coefficient in steady and transient states. The major advantage of the inverse method is that it can be carried out with simple, low cost experimental equipment. A study of sensitivity coefficients and a choice of how much bias and variance error is acceptable can be a good start in designing the optimal experiment. Due to the existence of lateral conduction within stainless steel, the local heat transfer coefficient was corrected to include this effect. The correction was performed regarding a two-dimensional model. It can be also be concluded that the two dimensional IHCP method (sequential function specification method and conjugate gradient method), especially with mollified measurement data, can suitably be used to design optimum simulation of convective heat transfer coefficient estimation before

doing the actual experiment. The temperature measurements are assumed to contain the major sources of error or uncertainty. Any known systematic effects due to calibration errors, presence of sensor, conduction and convection losses, or whatever, are assumed to be removed to the extent that the remaining errors may be considered random. It can be seen that by using the mollification method for smoothing measurement data before the IHC algorithm, fluctuations in the estimated parameter are reduced and the estimation is more accurate.

Nomenclature

A	Vector of unity matrices
D	Bias error
h	Heat transfer coefficient (W/m^2K)
H	Nozzle-to-plate distance
H/D	h nozzle-to-plate spacing ratio
K	Thermal conductivity (W/m.K)
L_1	Half-plate length
L_2	plate thickness
M	Time index
N	Number of discrete measurements
Np	Number of unknown parameters
Ns	Number of sensors
q	Heat flux vector (W/m^2)
Q_s	Heat flux subjected on top surface(W/m^2)
r	Number of future time steps
RMS	Root Mean Square error
S	Sum of squares (K^2)
d	Conjugate direction
T	Vector of calculated temperatures
V	Variance error
W	Slot width
X	Sensitivity coefficient matrix (K/W)
x, y	Space coordinates
Y	Measured temperature
Z	XA

Greek symbols

α	Thermal diffusivity (m^2/s)
σ	Standard deviation of noise
β	Search step size
γ	Conjugate coefficient
ε	Noise value

Subscripts

0	Initial state
j	Position index
jet	Jet exit
meas	Measured
surf	Impingement surface

Acknowledgements

This work was partially supported by the Iranian Gas Transmission Company and the Center of Excellence in Design and Optimization of Energy Systems (CEDOES).

References

1. Choom K.S. and Jim, S.J. "Comparison of thermal characteristics of confined and unconfined impinging jets", *Int. J. of Heat and Mass Transfer*, **53**, pp. 3366-3371 (2010).
2. Koseoglu, M.F. and Baskaya, S. "The role of jet inlet geometry in impinging jet heat transfer: Modeling and experiments", *Int. J. of Thermal Sciences*, **49**, pp. 1417-1426 (2011).
3. Kottke, V. and Geschwind, P. " Heat and mass transfer along curved walls in internal flows", *ERCOFTAC Bull*, **32**, pp. 21-24 (1997).
4. Krückels, S.W. and Kottke, V. "Investigation of the distribution of heat transfer on fins and finned tube models", *Chem. Eng. Technol.*, **42**, pp. 355-362 (1970).
5. Baughn, J.W., Mayhew, J.E., Anderson, M.R. and Butler, R.J. "A periodic transient method using liquid crystals for the measurement of local heat transfer coefficients", *J. Heat Transfer*, **119**, pp. 242-248 (1998).
6. Wang, Z., Ireland, P.T., Jones, T.V. and Davenport, R. "A color image processing system for transient liquid crystal heat transfer experiments", *J. Turbomach*, **118**, pp. 421-427 (1996).
7. Smits, A.J. and Lim, T.T. *Flow Visualization: Techniquesand Examples*, Imperial College Press, Singapore, Eds. (2003).
8. Ervin, J., Bizzak, D.J., Murawski, C., Chyu, M.K. and MacArtur, C. "Surface temperature determination of a cylinder in cross flow with thermographic phosphors", *Visualization of Heat Transfer Processes, The American Society of Mechanical Engineers*, New York, HTD, **252**, pp. 1070-1076 (1992).
9. Merski, N.R. "Global aero heating wind-tunnel measurements using improved two-color phosphor thermography method", *J. Spacecr Rockets*, **36**, pp. 160-170 (1999).
10. Liu, T. and Sullivan, J.P., *Pressure and Temperature Sensitive Paints*, Springer, Berlin (2005).

11. Lee, D.H., Bae, J.R., Park, J.S., Lee, J. and Ligrani, P. "Confined, milliscale unsteady laminar impinging slot jets andsurface Nusselt numbers", *Int. J. of Heat and Mass Transfer*, **54**, pp. 2408-2418 (2011).

12. Narayanan, V., Seyed-Yagoobi, J. and Page, R.H. "An experimental study of fluid mechanics and heat transfer in an impinging slot jet flow", *Int. J. of Heat and Mass Transfer*, **47**, pp. 1827-1845 (2007).

13. Hadamard, J. *Lectures on Couchy's Problem in Linear Differential Equations*, Yale University Press, New Haven, CT (1923).

14. Tikhonov, C.R. St. "Inverse problems in heat conduction", *J. Eng. Phys.*, **29**, pp. 816-820 (1975).

15. Beck, J.V., Blackwell, B. and Clair, C.R. St. *Inverse Heat Conduction: Ill-Posed Problems*, Wiley Interscience, New York (1985).

16. Baonga, J.B., Louahlia-Gualous, J.B. and Imbert, M. "Experimental study of hydrodynamic and heat transfer of free liquid jet impinging a flat circular heated disk", *Appl. Thermal Eng.*, **26**, pp. 1125-1138 (2005).

17. Masson, P.L., Loulou, T. and Artioukhine, T. "Estimation of a 2D convection heat transfer coefficient during a test: Comparison between two methods and experimental validation", *Inv. Probl. Sci. Eng.*, **12**, pp. 595-617 (2004).

18. Taler, J. "Determination of local heat transfer coefficient from the solution of the inverse heat conduction problem", *Forsch. Ingenieurwes.*, **71**, pp. 69-78 (2007).

19. Guzik, A. and Styrylska, T. "An application of the generalized optimal dynamic filtration method for solving inverse heat transfer problems", *Numerical Heat Transfer Part A*, **42**, pp. 531-548 (2002).

20. Kowsary, F. and Farahani, S.D. "the smoothing of temperature data using the mollification method in heat flux estimating", *Numerical Heat Transfer, Part A*, **58**, pp. 227-246 (2010).

21. Anantawaraskul, S. "Heat transfer enhancement under a turbulent impinging slot jet", Ph.D. Thesis, McGill University, Montreal, Quebec, Canada (2000).

Biographies

Somayeh Davoodabadi Farahani is a PhD degree student in the field of heat transfer at the University of Tehran, Iran. Her research interests include the use of numerical and analytical methods for solution of heat transfer problems, direct simulation of thermal systems, solution of inverse heat transfer problems, optimization of thermal systems, nanofluid and nanoscale heat transfer.

Farshad Kowsary is Professor in the field of heat transfer at the University of Tehran, Iran. His research interests include inverse heat transfer with a focus on inverse radiation and conduction. He has published several papers in these subjects in reputable heat transfer journals, and is a major reviewer for the Journal of Quantitative Spectroscopy and Radiative Transfer and the Journal of Heat and Mass Transfer.

Jalil Jamali is Assistant Professor in the field of heat transfer at Islamic Azad University, Shoushtar, Iran. His research interests include mathematics, fluid mechanics, acoustics (wave scattering) and elastodynamics